Available online at www.sciencedirect.com

SciVerse ScienceDirect

Ceramics International 38 (2012) 4525–4532

CERAMICS INTERNATIONAL

www.elsevier.com/locate/ceramint

Inactivation of pathogenic *Klebsiella pneumoniae* by CuO/TiO_2 nanofibers: A multifunctional nanomaterial via one-step electrospinning

Ayman Yousef [a], Nasser A.M. Barakat [b,c,*], Touseef Amna [d], Salem S. Al-Deyab [e], M. Shamshi Hassan [b], Abdallah Abdel-hay [a], Hak Yong Kim [b,d,**]

[a] *Bionano System Engineering Department, Chonbuk National University, Jeonju 561-756, South Korea*
[b] *Organic Materials and Fiber Engineering Department, Chonbuk National University, Jeonju 561-756, South Korea*
[c] *Chemical Engineering Department, Faculty of Engineering, Minia University, El-Minia, Egypt*
[d] *Centre for Healthcare Technology Development, Chonbuk National University, Jeonju 561-756, South Korea*
[e] *Petrochemical Research Chair, Department of Chemistry, College of Science, King Saud University, Riyadh 11451, Saudi Arabia*

Received 1 February 2012; accepted 10 February 2012
Available online 19 February 2012

Abstract

The fabrication and characterization of one-dimensional CuO/TiO_2 nanofibers with high photocatalytic and antibacterial activities are presented. The CuO/TiO_2 nanofibers were prepared by electrospinning of colloid composed of titanium isopropoxide, poly(vinylpyrroliodine) (PVP) and copper nanoparticles and calcination at 700 °C in air for 1 h. The antibacterial activity was tested using *Klebsiella pneumoniae* as model organism by calculation of the minimum inhibitory concentration (MIC). The obtained CuO/TiO_2 nanofibers showed prominent photocatalytic activity under visible light to degrade reactive black5 and reactive orange16 dyes in aqueous solutions and effectively catalyze *K. pneumoniae* inactivation. The decomposition process of the cell wall and cell membrane was directly observed by TEM analysis after the exposure of the *K. pneumoniae* to the nanofibers. Interestingly, the introduced photocatalyst can be reused with the same photocatalytic activity. Overall, the combination of CuO and TiO_2 can be synergistic and resulted in CuO/TiO_2 composite nanofibers having superior photocatalytic and antimicrobial potential to impede *K. pneumoniae* growth which causes bacterium to die ultimately.

Keywords: Photocatalytic activity; *Klebsiella pneumoniae*; Antibacterial activity; CuO/TiO_2 nanofibers

1. Introduction

Microbial contamination possesses a major threat to public health. *Klebsiella pneumoniae* is a Gram-negative, non-motile, encapsulated, facultative anaerobic bacterium found in the normal flora of the mouth, skin, and intestines. Clinically, it is the most important member of the *Klebsiella* genus of Enterobacteriaceae and is responsible for various human infectious diseases in immunocompetent individuals. *Klebsiella* is well known to most clinicians as a cause of community acquired bacterial pneumonia. The *Klebsiella* spp. is opportunistic pathogens, so primarily attack immunocompromised individuals are hospitalized and suffer from severe underlying diseases [1]. Nosocomial Klebsiella infections are caused mainly by *K. pneumoniae*, the medically most important species of the genus. Transmission of nosocomial outbreak related bacteria may be effectively controlled by taking appropriate control measures. The emergence of antibiotic resistance among pathogens has revived the interest of the scientific community in alternative methods of reducing bioburden in healthcare facilities; particularly hospitals and to search new cost-effective drugs of natural or synthetic origin [2,3]. The use of metal oxides as antimicrobial agents has numerous benefits such as improved safety and stability, as compared to the organic antimicrobial agents [4]. Recently, nanofibers have attracted a lot of attention due to the huge potential for a wide range of applications. The expanding applications include tissue engineering, biomaterials, nanocomposites, filtration and drug delivery [5–7]. Though

* Corresponding author at: Organic Materials and Fiber Engineering Department, Chonbuk National University, Jeonju 561-756, South Korea. Tel.: +82 632702363; fax: +82 632702348.
** Corresponding author at: Centre for Healthcare Technology Development, Chonbuk National University, Jeonju 561-756, South Korea.
E-mail addresses: nasser@jbnu.ac.kr (N.A.M. Barakat), khy@jbnu.ac.kr (H.Y. Kim).

0272-8842/$36.00
doi:10.1016/j.ceramint.2012.02.029

several TiO_2 nanocomposites with antimicrobial capabilities have been reported, there are still barriers in their antibacterial application under dark conditions. It has been known that pure TiO_2 exhibits low photocatalytic property due to rapid recombination of the photoactivated electrons and holes. Doping with metal or metal oxide shows an improvement of photocatalytic activity and disinfection effect. As previously reported, doping TiO_2 with metallic ions or oxides such as Fe^{3+}, Ag, or SnO_2 enhances the photocatalytic activity and bacteria killing effect [8–10]. In this study we present the effect of Cu doping in TiO_2 nanofibers on the photocatalytic activity and disinfection of *K. pneumoniae*. Copper ions have been reported to have antimicrobial activity against a wide range of microorganisms' viz., *Salmonella enterica, Campylobacter jejuni, Escherichia coli, Listeria monocytogenes*, and S*taphylococcus aureus* [11–13]. It is one of the relatively small groups of metallic elements essential to human health. The copper is considered safe to humans since it is used in the intrauterine devices [14]. Though copper is also required in trace amounts for the growth of microorganisms; however, higher concentrations can produce a toxic effect [15]. The objective of our study was thus determining the photocatalytic activity of the fabricated Cu-doped TiO_2 nanofibers and to establish a concentration of Cu-doped TiO_2 that effectively inhibits the growth of in *K. pneumoniae* in nutrient medium.

2. Experimental

2.1. Materials

Titanium isopropoxide ($Ti(OiPr)_4$), poly(vinyl pyrrolidone) (PVP), and copper(II) acetate hydrate (CuAc) (assay 98%) were purchased from sigma Aldrich. Copper powder (CuNPs) (Cu, 99.9% purity analytical grade) was obtained from Osaka Chemicals Ltd., Japan. Reactive black 5 (RB) and Reactive orange16 (RO) dyes were obtained from sigma Aldrich. Analytical grade ethanol was used as the solvent. Trypton soy broth was purchased from Torlak, Belgrade and the tested strain *K. pneumoniae* KCCM 35454 was purchased from Korean Culture Centre of Microorganisms (KCCM). All the materials were used without any further purification.

2.2. Fabrication of Cu doped titania nanofibers

The titania nanofibers and Cu-doped titania nanofibers were prepared by sol–gel process. Titanium isopropoxide, poly(vinyl pyrrolidone) (PVP), copper(II) acetate hydrate (CuAc) and CuNPs were used as precursors. Typically to prepare pristine TiO_2 nanofibers, 1 g titanium isopropoxide $Ti(OiPr)_4$ was added to a solution containing 2 g acetic acid and 2 g ethanol followed by stirring for 15 min, then 6 g ethanol and 1 g PVP were added to titanium isopropoxide–acetic acid–ethanol solution and stirred until getting transparent sol–gel. Two different Cu precursors were utilized separately to prepare the Cu-doped TiO_2 nanofibers; copper acetate and Cu NPs. For a similar composition sol–gel used to prepare the pristine TiO_2 nanofibers, 0.05 g Cu NPs and 0.14 g copper acetate (dissolved in 2 ml ethanol) were added. Actually, these amounts of Cu NPs and CuAc were chosen to produce same CuO content in the produced nanofibers. Upon good mixing, the colloidal and transparent solutions were obtained. The obtained sol–gels and colloidal solution were drawn individually into a plastic syringe attached to a capillary tip for electrospinning. A positive electrode (anode) connected to a copper pin was inserted into the solution, and a negative electrode (cathode) was attached to stainless steel drum covered by poly(ethylene) sheet. The electrospinning process was carried out at 20 kV and a 15-cm working distance (the distance between the needle tip and the collector). The formed nanofiber mats were initially dried for 24 h at 60 °C under vacuum and then calcined in air at 700 °C for 1 h, with a heating rate of 5 °C/min, and finally cooled to room temperature.

2.3. Antibacterial assay

The antibacterial activity of CuO/TiO_2 nanofibers was studied using the growth inhibition studies against pathogenic organism *K. pneumoniae*. The inocula were prepared from fresh overnight broth culture (Trypton soy broth; pH 7.3) that was incubated at 37 ± 1 °C. Briefly, the bacterial strain was first grown on solid nutrient agar, fresh colonies were inoculated into 100 ml of broth medium. Growth was monitored at every 3 h by UV–Vis spectrophotometer till the optical density reached 0.1 at 600 nm (OD of 0.1 corresponded to a concentration of 10^8 CFU/ml of medium). Subsequently, 1 ml from the above was further added to 100 ml of freshly prepared nutrient broth medium supplemented with 0, 5, 15, 25, 35 and 45 μg/ml of CuO/TiO_2 nanofibers solutions. Control broth solution without nanofibers was also kept. All the flasks were incubated at 37 ± 1 °C in a rotary shaker with shaking at 150 rpm. The growth rate and the bacterial concentration were monitored by measuring the optical density (OD) at 600 nm by UV-spectrophotometer at an interval of 4 h for 20 h.

2.4. Visible light photocatalytic activity test

The Photo catalytic degradation of the RB and RO were carried out in a simple photo reactor. The reactor was made of simple laboratory glass bottle 70 ml capacity. The photocatalytic degradation was carried out under radiation of Philips projection lamp (7748XHP 250 W, 532 nm). In each experiment, 50 ml (10 ppm) dye aqueous solutions and 25 mg of the catalyst were added to the bottle, the colloid was magnetically stirred under the utilized visible light radiation. At specific time intervals, a 2 ml sample was taken out and centrifuged to separate the residual nanofibers catalyst. The concentration of the dye in the withdrawn samples was investigated using UV–Vis spectrophotometer. The calibration curves for reactive black 5 and reactive orange 16 dyes were firstly constructed by measuring the absorbance at different concentrations.

2.5. Characterization

The surface morphology of the as-obtained nanofibers was studied by a JEOL JSM-5900 scanning electron microscope

(equipped with EDX) (JEOL Ltd., Japan) and field-emission scanning electron microscope (FESEM, Hitachi S-7400, Japan). The phase and crystallinity of the catalyst were characterized using a Rigaku X-ray diffractometer (Rigaku Co., Japan) with Cu Kα (λ = 1.54056 Å) radiation over a range of 2θ angles from 10° to 80°. High-resolution images and selected area electron diffraction patterns were observed by a JEOL JEM-2200FS transmission electron microscope (TEM) operating at 200 kV (JEOL Ltd., Japan). The concentration of the dyes during the photo degradation study was investigated by spectroscopic analysis using a HP 8453 UV–Vis spectroscopy system (Germany). The spectra obtained were analyzed by a HP ChemiStation software5890 series.

3. Results and discussion

3.1. Phase morphology

Electrospinning process can be sustained in a variety of modes characterized by the shape of the surface from which the liquid jet originates [16]. Fig. 1A–C shows the SEM images of $Ti(OiPr)_4$/PVP, CuAC/$Ti(OiPr)_4$/PVP, and Cu NPs/$Ti(OiPr)_4$/PVP electrospun nanofibers after drying at 60 °C for 24 h, respectively. As shown in these figures, nanofibers having good morphology were obtained with all formulations. The average diameter was estimated to be about 213, 181 and 241 nm for the $Ti(OiPr)_4$/PVP, CuAC/$Ti(OiPr)_4$/PVP and Cu NPs/$Ti(OiPr)_4$/PVP nanofibers, respectively. Smooth and continuous nanofibers in random orientation due to the bending instability accompanied with the spinning jet can be observed in all figures. Fig. 1D–F reveal the SEM images of the obtained powder from each formulation after the calcination process. As shown in Fig. 1D which represents the powder obtained from calcination of $Ti(OiPr)_4$/PVP, good nanofibers morphology was obtained with an average diameter of 115 nm. Addition of cooper acetate as a copper precursor had a bad impact on the nanofibrous morphology as it completely destroyed the 1D structure as shown in Fig. 1E. However, Cu NPs revealed good performance as good morphology nanofibers with an average diameter of 130 nm were obtained from calcination of Cu NPs/Ti(OiPr)4/PVP electrospun mat (Fig. 1F). Decrease in the average diameters of the sintered nanofibers might be due to elimination of the polymer by calcination the samples at utilized temperature [17]. The increase in the average diameter of the Cu-containing nanofibers as compared with Cu-free ones may be resulted from embedding of CuO NPs. Fig. 1G–I. reveal

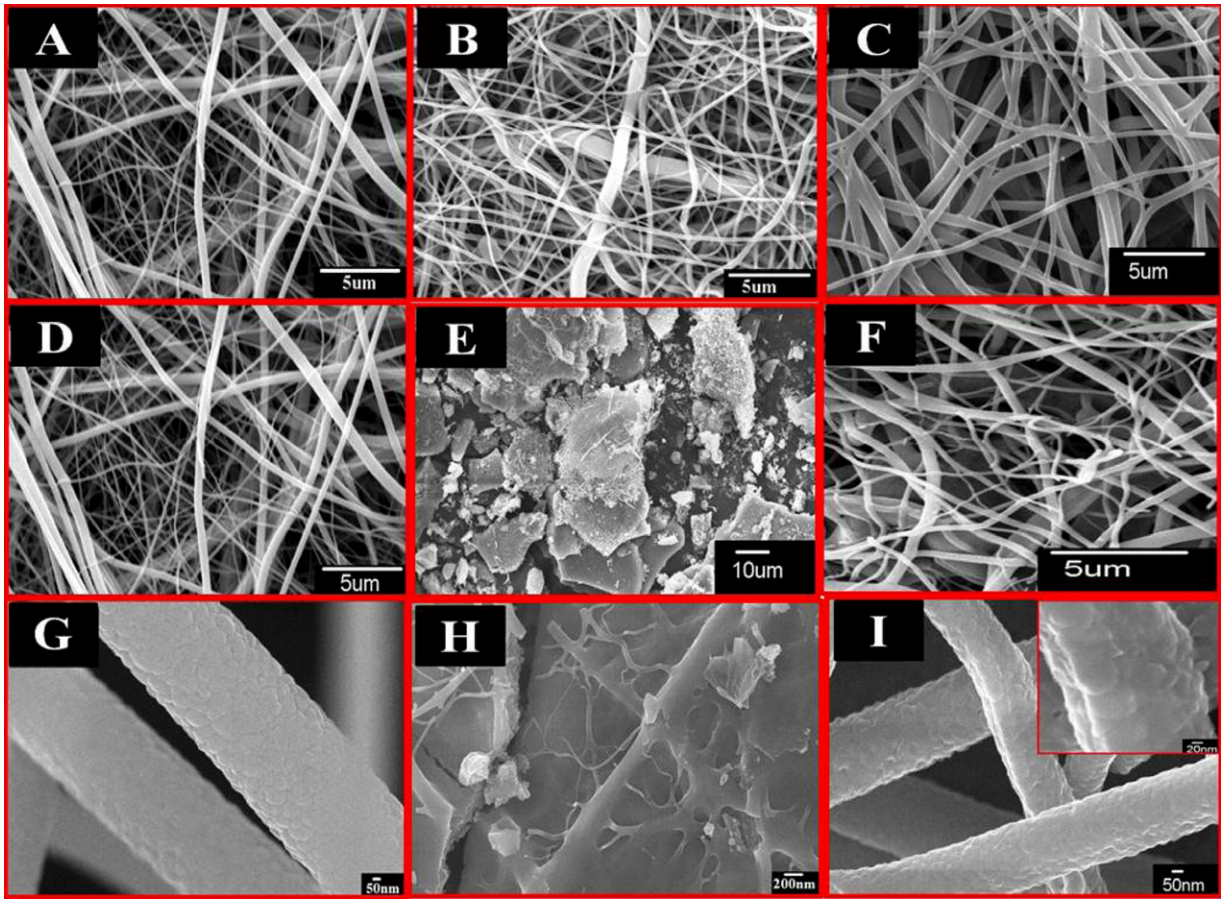

Fig. 1. SEM images of the nanofibers after drying at 60 °C for 24 h (A) $Ti(OiPr)_4$/PVP mat, (B) CuAc/$Ti(OiPr)_4$/PVP mat, and (C) Cu NPs/$Ti(OiPr)_4$/PVP mat. Panels D–I represent SEM and FE SEM images of the produced nanofibers after calcination of $Ti(OiPr)_4$/PVP mat; (D and G), CuAc/$Ti(OiPr)_4$/PVP mat; (E and H) and Cu NPs/$Ti(OiPr)_4$/PVP mat; (F and I) at 700 °C for 1 h.

FE-SEM images for all formulations, it can be seen a smooth surface in the case of Cu-free nanofibers (Fig. 1G) and slightly rough one for Cu-doped nanofibers (Fig. 1I).

3.2. Phase structure

To understand the crystal structure of the obtained nanofibers, XRD analysis was carried out. Fig. 2 demonstrates the XRD patterns of produced nanofibers. As shown in this figure, the XRD analysis reveals the presence of anatase and rutile phases in both formulations in addition to CuO in the copper-containing nanofibers. It is clearly observing the rutile phase with a tetragonal structure (space group *P*42/*mnm* (136), JCPDS 21-1276) at 2θ values 27.4°, 36.1°, 39.2°, 41.2°, 44.1°, 54.3°, 56.6°, 62.7°, 64.00°, 69.00°, and 69.8° that corresponding to (1 1 0), (1 0 1), (2 0 0), (1 1 1), (2 1 0), (2 1 1), (2 2 0), (0 0 2), (3 1 0), (3 0 1), and (1 1 2) crystal planes, respectively. In the same spectra, anatase phase with a tetragonal structure (space group 141/*amd* (141), JCPDS 21-1272) peaks at 2θ values 25.2°, 37.8°, 38.6°, 48°, 62.7°, and 75.00° that corresponding to (1 0 1), (0 0 4), (1 1 2), (2 0 0), (2 0 4), and (2 1 5) crystal planes, respectively can be detected. Also, the diffraction pattern of monoclinic crystal structure of CuO (Tenorite) phase (space group *C*2/*C*(15), JCPDS 05-066) peaks at 2θ values 32.5°, 35.5°, 38.7°, 48.7°, 58.3°, 61.5°, 65.8°, 66.2°, 68.1°, 72.4°, and 75.00° that corresponding to (1 1 0), (−1 1 1), (1 1 1), (−2 0 2), (2 0 2), (−1 1 3), (0 0 2), (−3 1 1), (2 2 0), (3 1 1), and (0 0 4), respectively are shown in the nanofibers prepared by addition of the Cu NPs to the prepared sol–gel. The energy dispersive X-ray spectroscopic analysis of the doped oxide confirms the presence of Ti; Cu and O elements in the spectrum and the counted percentages of the elements were 42.43, 3.34, and 54.22 for Ti, Cu and O, respectively, which agrees with the stoichiometry (Fig. 2B). To obtain the microstructure of the CuO/TiO2 nanofibers, TEM analysis

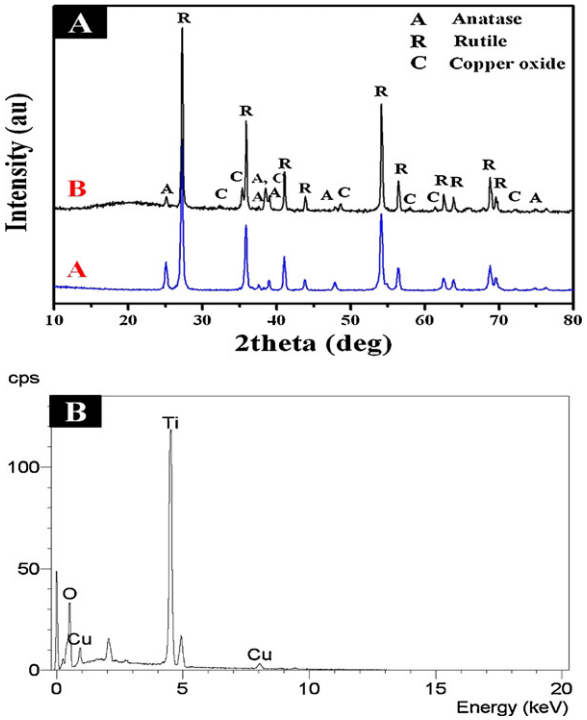

Fig. 2. (A) XRD patterns of the nanofibers obtained after calcination CuNPS/Ti(OiPr)$_4$/PVP at 700 °C for 1 h in air, (B) EdS spectrum of the produced nanofibers.

was invoked. The TEM images shown in Fig. 3 provide a clear observation of the as-synthesized CuO/TiO$_2$ nanofibers. From Fig. 3A which represents the normal TEM image, it could be seen that the surface is smooth with a diameter about 115 nm; which is consistent with the SEM results. Also, black nanoparticles may be corresponded to CuO can be seen. High-resolution TEM image of the marked area in Fig. 3A is shown in Fig. 3B, this image indicates the presence of parallel atomic planes and reveals excellent crystallinity of the obtained

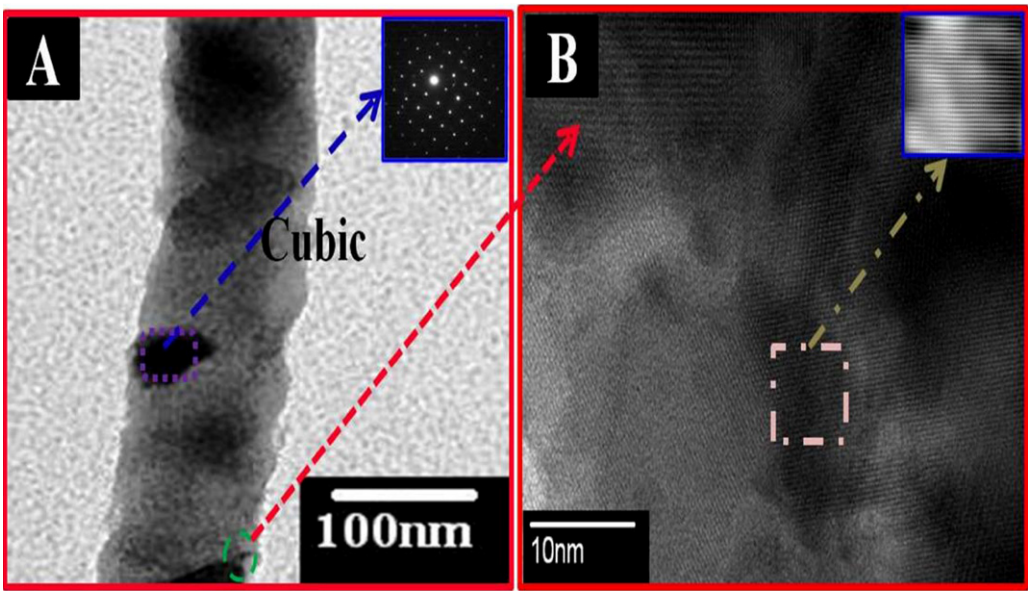

Fig. 3. TEM image; (A) and HR TEM; (B) for the marked area by the green circle in A. The insets in panels A and B represent the SAED pattern and FFT image for the marked areas, respectively. (For interpretation of the references to color in this figure legend, the reader is referred to the web version of the article.)

nanofibers. The inset in Fig. 3A represents the SAED pattern, one can claim that this part represents CuO as the planar distance almost matches the standard value for the CuO, moreover a good crystallinity without any defects can be observed for the marked portions.

3.3. Photoluminescence (PL) study

The PL emission spectra were used to reveal the efficiency of trapping, migration, transfer and separation of charge carriers, and to investigate their lifetime in semiconductor since PL emission results from the recombination of electron/hole pairs [18]. Fig. 4 shows comparison PL spectra at an excitation wavelength 320 nm for TiO_2 and Cu-doped TiO_2 nanofibers in the wavelength range of 400–600 nm obtained at the same experimental conditions. As shown in the figure, the first parts (from 420 to ~470 nm), the two spectra are almost similar so it can be said that these zones demonstrate the TiO_2 in the nanofibers [19]. An additional peak can be observed at ~590 nm for the CuO-containing nanofibers; this peak affirms presence of CuO [20] and simultaneously supports the utilized characteristics techniques. PL analysis provides an important finding about addition of CuO to TiO_2, the former leads to decrease the PL intensities for the new composite. A lower PL intensity indicates a lower recombination rate of the excited electrons/holes and low defects in the produced nanofibers [21]. In other words, lower PL intensity indicates low recombination rate which is preferable in case of utilizing the materials as catalysts in the photoreactions. This is mainly due to the fact that the electrons are excited from the valance band to the conduction one of TiO_2 and then transfer to CuO nanoparticles, which prevent the direct recombination of electrons and holes.

3.4. Antibacterial activity of Cu-doped TiO_2 nanofibers

The growth curves of *K. pneumoniae* treated with CuO/TiO_2 nanfibers was shown in Fig. 5 by measuring the optical density at 600 nm. In presence of 0, 5, 15, 25, 35 and 45 μg/ml of CuO/TiO_2 nanofibers solution, the growth curve of tested strain included three phases: lag phase, exponential phase, and stabilization phase. However, decline and death phase in growth curve could not be revealed as we only assayed the total numbers of bacteria, including live and dead ones, based on the value of OD_{600}. In the absence of CuO/TiO_2 nanofibers, the organism reached exponential phase rapidly. But upon exposure to different concentrations of electrospun fibers, *K. pneumoniae* cells were lagged. With the increasing concentration of the synthesized nanofibers, the delay was more evident. CuO/TiO_2 nanofibers exhibit excellent antibacterial performance against *K. pneumoniae* and it has been seen that with increase the concentration of CuO/TiO_2 nanofibers, the inhibition has also increased. Noticeable difference in the growth rate has been observed compared to the control cells. The higher concentrations (35 and 45 μg/ml) of CuO/TiO_2 solution has been found to exhibit excellent toxicity against the tested pathogenic strain. The electron micrographs by TEM of *K. pneumoniae* cells treated with CuO/TiO_2 were displayed in Fig. 6. Micrograph (inset) showed the untreated surfaces of *K. pneumoniae* cells are smooth and with intact morphology, while cells treated with CuO/TiO_2 nanofibers are misshapen (Fig. 6B) and severely damaged (Fig. 6C).

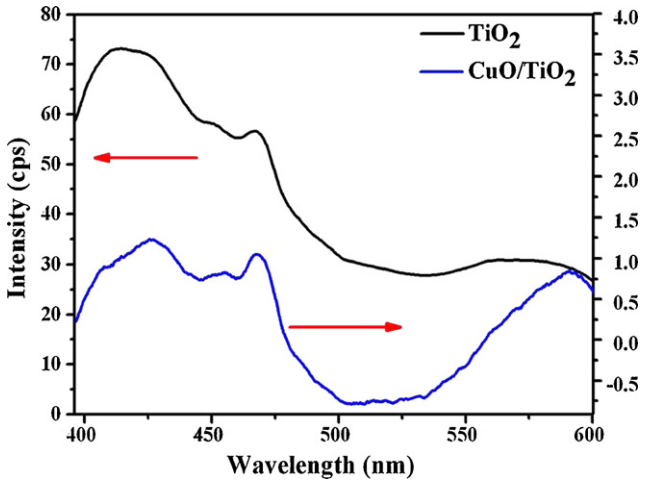

Fig. 4. Room temperature photoluminescence spectrum of prepared TiO_2 and CuO/TiO_2 nanofibers.

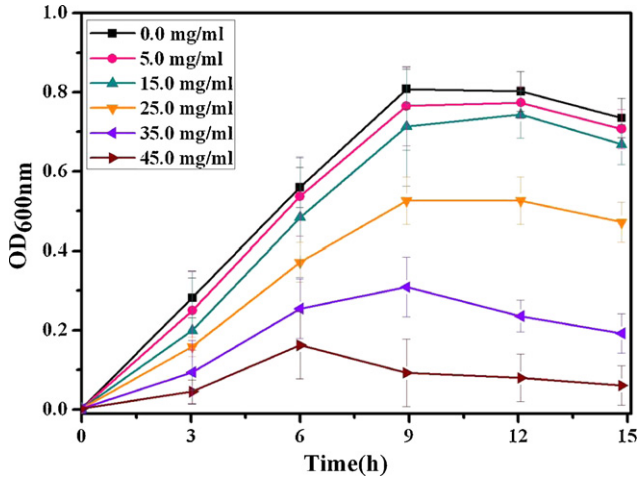

Fig. 5. Growth curves of *K. pneumoniae* exposed to different concentrations of CuO/TiO_2 nanofibers.

3.5. De-coloration of RB and RO dyes from water

According to many reports, the azo dyes are difficult to be completely eliminated using the conventional photocatalyst. In this study, the as-obtained nanofibers were examined to treat two azo dyes; reactive black 5(RB) and reactive orange16 (RO) under the visible light radiation, the results demonstrated in Figs. 7 and 8. As shown in these figures, fast and complete oxidation of both dyes was achieved which strongly recommends utilizing of the proposed nanofibers to treat various kinds of organic pollutants. The result appeared fast degradation for the azo dyes under the normal visible light radiation by using Cu-doped TiO_2 nanofibers as compared with TiO_2 nanofibers. This result confirms the PL data and clarifies the conflict between this study and the previously reported ones

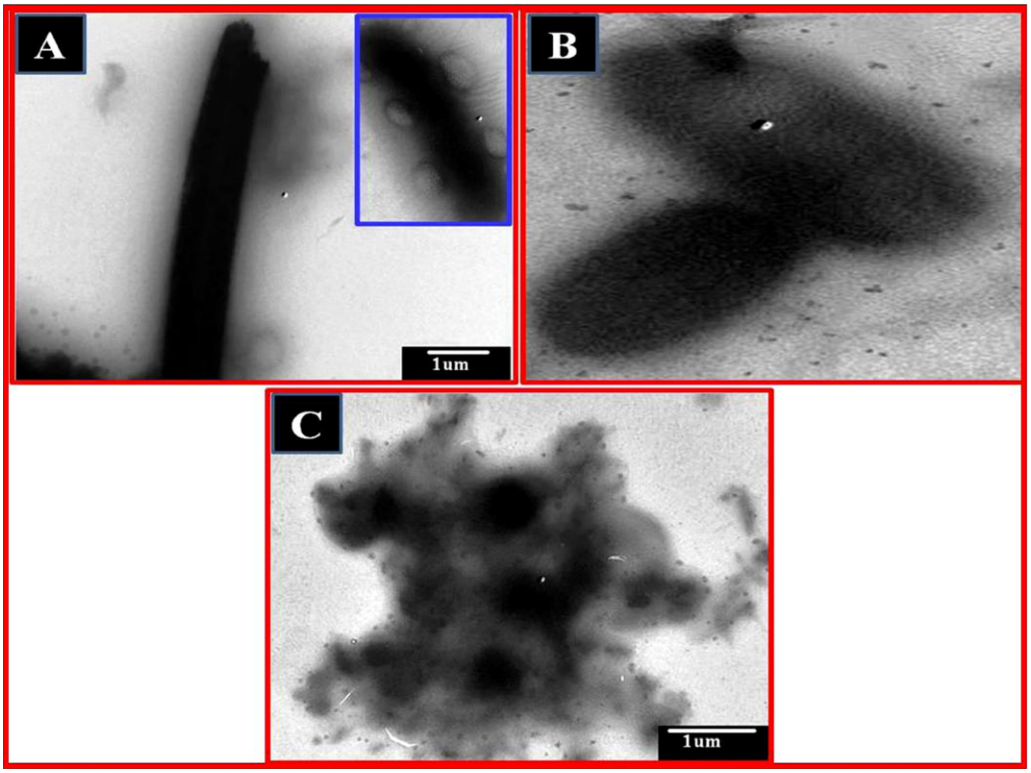

Fig. 6. Representative transmission electron microscope images of *K. pneumoniae* exposed to CuO/TiO_2 nanofibers (inset native *K. pneumoniae*).

concluding that TiO_2 can be utilized as photocatalyst only under UV light [22,23]. Interestingly, the introduced CuO/TiO_2 nanofibers can be reused without any effect on their photocatalytic efficiency.

3.6. Mechanism of photocatalytic degradation of RB and RO, and disinfection of K. pneumoniae

Fig. 9A indicates the mechanism for the charge transfer and separation that supports the high photocatalytic activity of the coexistence of TiO_2 and CuO under visible light radiation. The photocatalytic de-colorization of reactive black 5(RB) and reactive orange16 (RO) in aqueous solutions is caused by the photoexcitation of CuO/TiO_2 nanofibers under visible light energy that leading to easily transfer of the excited electrons from the conduction band (CB) of TiO_2 to the CB of CuO because the conduction band of CuO ($E_{CB} = -4.96$ eV) is lower than that of conduction band of TiO_2 ($E_{CB} = -4.21$ eV). That is, Cu^{2+} may accept an electron to form Ti^{3+}. Also, the valence band (VB) of TiO_2 ($E_{VB} = 7.71$ eV) is more anodic than that of CuO ($E_{VB} = -6.66$ eV). This may also lead to holes transfer from the VB of TiO_2 to the VB of CuO [24] resulting in

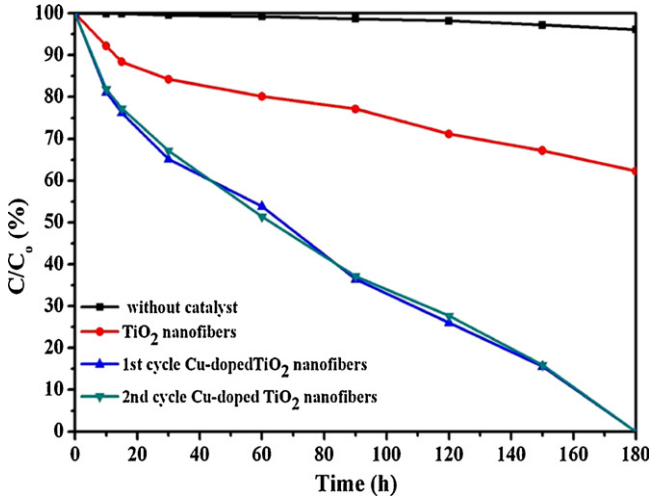

Fig. 7. Degradation profile of the RB dye under visible light by using TiO_2 and CuO/TiO_2 nanofibers.

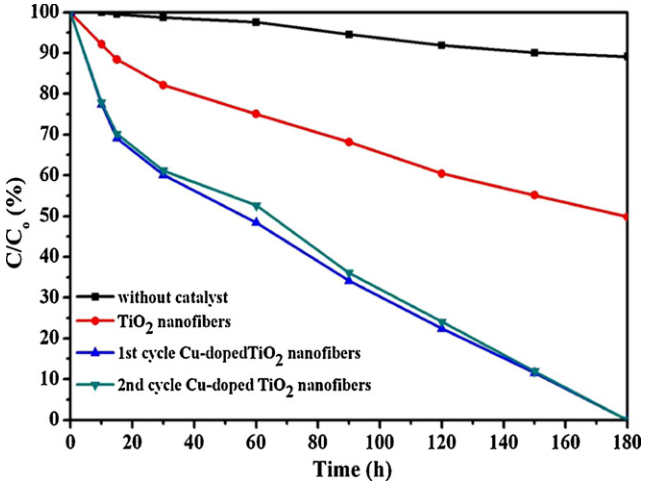

Fig. 8. Degradation profile of the RO dye under visible light by using TiO_2 and CuO/TiO_2 nanofibers.

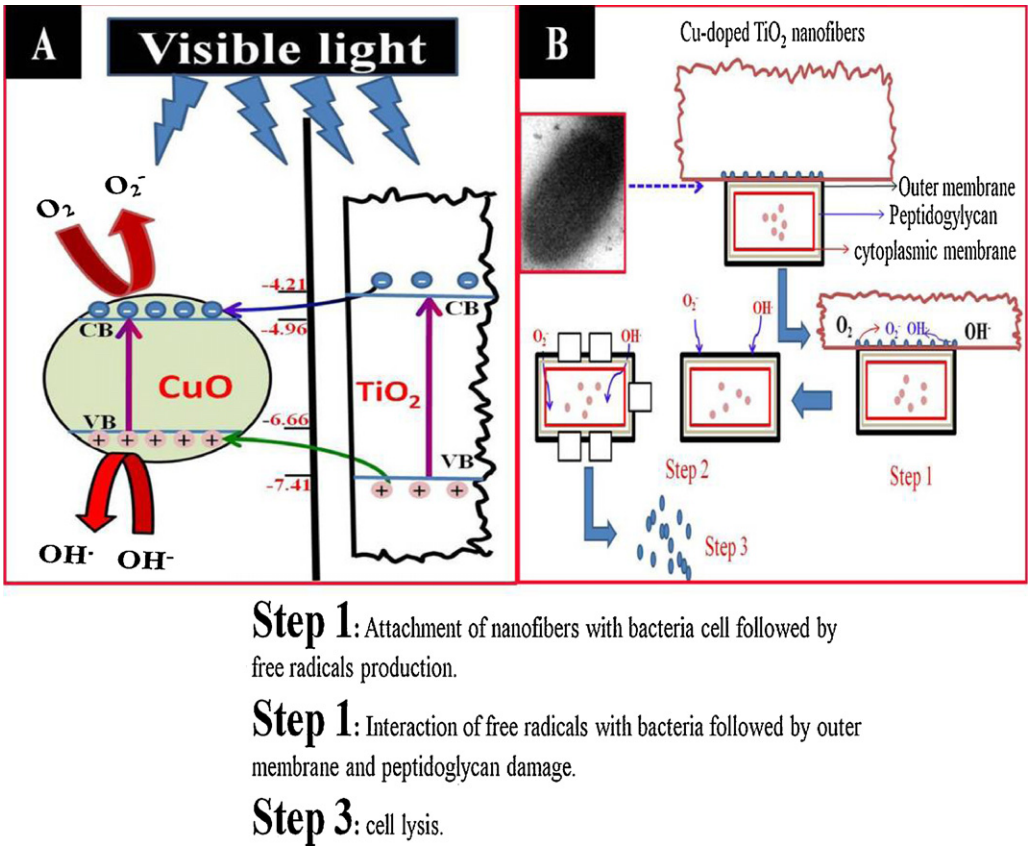

Fig. 9. Schematic diagram; (A) indicating the proposed mechanism for the photocatalytic of dye degradation under visible light, and (B) a proposed mechanism for the antibacterial activity of the introduced CuO/TiO_2 nanofibers.

a build up of excess electrons in the conduction band of CuO, which led to shift in the Fermi level of CuO [19]. The shift in the Fermi level is important for photocatalytic activity over CuO/TiO_2. These excess electrons in the conduction band of CuO will react with O_2 to produce $O_2^{\bullet -}$. Also, the holes which left in the valence band of CuO will react with H_2O or OH^- to produce active species such as $OH^{\bullet}$. This explanation is adequate to explain the decrease in the intensties in the PL spectra due to CuO incorporation. The efficient of the electron–hole separation could increase the lifetime of the charge carries which enhances the participation in the chemical reactions. The mechanism of formation of the free radicals can be suggested as follows:

At the conduction band

$$e^- + O_2 \rightarrow O^-{}_2$$

$$O^-{}_2 + O_2 \rightarrow HO^\circ{}_2 + OH^-$$

$$HO^\circ{}_2 + H_2O \rightarrow H_2O_2 + HO^\circ$$

$$H_2O_2 \rightarrow 2OH^\circ$$

At the valence band

$$h^+ + OH^- \rightarrow OH^\circ$$

The degradation efficiency of RB and RO solution was calculated to be about 100% using CuO/TiO_2 nanofibers within 3 h in visible light irradiation which indicates good formation of the active radicals.

We speculate the mechanism of disinfection of *K. pneumoniae* as the mechanism of degradation of the organic dye by CuO/TiO_2 nanofibers under normal light illumination. The first step is a formation of O_2^- and OH radical. Gram-negative bacteria including *K. pneumoniae* exhibit only a thin peptidoglycan layer between the cytoplasmic membrane and the outer membrane. Reactive species (O_2^-, $OH^{\bullet}$) attack the outer membrane and partially disintegrates the intact structure of the membrane. Furthermore, we assume that when the synthesized CuO/TiO_2 nanofibers were dispersed in the growth media the Cu^{2+} atoms present in these nanofibers interacted with the bacterial cells and adhered to the bacterial cell walls. The overall charge on the bacterial cell surface at biological pH values is negative, which is due to the excess number of carboxylic and other groups that upon dissociation make the cell surface negative [25]. Also the bacteria and the Cu^{2+} atoms in nanofibers have opposite charges, and these electrostatic forces may be the reason for their adhesion and bioactivity. The antibacterial activity of CuO/TiO_2 can be attributed to the damage of cell membranes, which leads to leakage of cell contents and ultimately cell death. Earlier, Nadtochenko et al. in their study described that though the cell membrane damage is known to result in cell death, a mechanism to repair cell wall damage does exist and therefore bacteria cell wall damage alone will not cause bacterial inactivation. The change in the

concentration of the cell wall components during illumination shows that while the outer membrane serves as a barrier, the peptidoglycan layer does not have a barrier function [26]. The photokilling reaction is initiated by a partial decomposition of the outer membrane followed by disordering of the cytoplasmic membrane resulting in cell death.

Beside the economic aspect of the introduced nanofibers due to the high photo catalytic activity in the visible light which will save the cost of UV, CuO/TiO_2 nanofibers could be easily separated and recovered by sedimentation due to insolubility in water, this leads to increase the practical application to remove the organic pollutants and microorganisms from the polluted water.

4. Conclusion

To incorporate CuO in TiO_2 nanofibers by the electrospinning process, Cu NPs can be added to the $Ti(OiPr)_4$/PVP sol–gel rather than utilizing copper acetate soluble precursor as the later leads to annihilate the one-dimensional structure. The introduced CuO/TiO_2 nanofibers show potent antimicrobial and photocatalytic activity. CuO can act as an effective co-catalyst to enhance the antimicrobial and photo catalytic properties of TiO_2. Copper oxide nanoparticles change the energy level and work as electron acceptor which favor the electron transfer and enhance the antimicrobial and photocatalytic activities. This study opens an avenue to the possibility of using CuO nanoparticles as a substitute for other materials invoked in the photocatalytic and antimicrobial purposes.

Acknowledgements

This paper was supported by research funds of Chonbuk National University 2010. The Authors extend their appreciation to the Deanship of Scientific Research at king Saud University for funding the work through the research group project No. RGP-VPP-089. We thank Mr. T. S. Bae, Mr. J. C. Lim, Dr. Lee Young-Boo, KBSI, Jeonju branch, and Mr. Jong-Gyun Kang, Centre for University Research Facility, for taking high-quality FESEM, TEM-EDX and TEM images, respectively.

References

[1] R. Podschun, U. Ullmann, Klebsiella spp. as nosocomial pathogens: epidemiology, taxonomy, typing methods, and pathogenicity factors, Clin. Microbiol. Rev. 11 (1998) 589–603.

[2] F. Gl, O. Ja, S. Kp, Tackling contamination of the hospital environment by methicillin resistant *Staphylococcus aureus* (MRSA): a comparison between conventional terminal cleaning and hydrogen peroxide vapour decontamination, J. Hosp. Infect. 57 (2004) 31–37.

[3] P. Mr, A. Ld, N. Udupa, Evaluation of antiplaque activity of Azadirachta indica leaf extract gel a 6-week clinical study, J. Ethnopharmacol. 90 (2004) 99–103.

[4] R. Brayner, R. Ferrari-Iliou, N. Brivois, S. Djediat, M.F. Benedetti, F. Fievet, Toxicological impact studies based on *Escherichia coli* bacteria in ultrafine ZnO nanoparticles colloidal medium, Nano Lett. 6 (2006) 866–870.

[5] A. Frenot, I.S. Chronakis, Polymer nanofibers assembled by electrospinning, Curr. Opin. Colloid Interface Sci. 8 (2003) 64–75.

[6] R. Nirmala, D. Kalpana, J.W. Jeongc, H.J. Oh, J.H. Lee, R. Navamathavan, Y.S. Lee, H.Y. Kim, Multifunctional baicalein blended poly(vinyl alcohol) composite nanofibers via electrospinning, Colloid Surf. A 384 (2011) 605–611.

[7] H.R. Panta, M.P. Bajgai, C. Yi, R. Nirmala, K.T. Nam, W.-i. Baek, H.Y. Kim, Effect of successive electrospinning and the strength of hydrogen bond on the morphology of electrospun nylon-6 nanofiber, Colloid Surf. A 370 (2010) 87–94.

[8] W. Zhang, Y. Chen, S. Yu, S. Chen, Y. Yin, Preparation and antibacterial behavior of Fe^{3+}-doped nanostructured TiO_2 thin films, Thin Solid Films 516 (2008) 4690–4694.

[9] O. Akhavan, Lasting antibacterial activities of Ag–TiO_2/Ag/a-TiO_2 nanocomposite thin film photocatalysts under solar light irradiation, J. Colloid Interface Sci. 336 (2009) 117–124.

[10] A. Rkan, U. Bakir, G. Karakas, Photocatalytic microbial inactivation over Pd doped SnO_2 and TiO_2 thin films, J. Photochem. Photobiol. A 184 (2006) 313–321.

[11] G. Faúndez, M. Troncoso, P. Navarrete, G. Figueroa, Antimicrobial activity of copper surfaces against suspensions of *Salmonella enterica* and *Campylobacter jejuni*, BMC Microbiol. 4 (2004) 4–19.

[12] S.A. Ibrahim, H. Yang, C.W. Seo, Antimicrobial activity of lactic acid and copper on growth of Salmonella and *Escherichia coli* O157: H7 in laboratory medium and carrot juice, Food Chem. 109 (2008) 137–143.

[13] S. Rodgers, E. Ryser, Reduction of microbial pathogens during apple cider production using sodium hypochlorite, copper ion, and sonication, J. Food Prot. 67 (2004) 766–771.

[14] G. Borkow, J. Gabbay, Copper as a biocidal tool, Curr. Med. Chem. 12 (2005) 2163–2175.

[15] J. Trevors, C. Cotter, Copper toxicity and uptake in microorganisms, J. Ind. Microbiol. Biotechnol. 6 (1990) 77–84.

[16] N.A.M. Barakat, K.D. Woo, M.A. Kanjwal, K.E. Choi, M.S. Khil, H.Y. Kim, Surface plasmon resonances, optical properties, and electrical conductivity thermal hystersis of silver nanofibers produced by the electrospinning technique, Langmuir 24 (2008) 11982–11987.

[17] M.P. Zheng, Y.P. Jin, G.L. Jin, M.Y. Gu, Characterization of TiO_2–PVP nanocomposites prepared by the sol–gel method, J. Mater. Sci. Lett. 19 (2000) 433–436.

[18] S. Xu, D.D. Sun, Significant improvement of photocatalytic hydrogen generation rate over TiO_2 with deposited CuO, Int. J. Hydrogen Energy 34 (2009) 6096–6104.

[19] J. Yu, Y. Hai, M. Jaroniec, Photocatalytic hydrogen production over CuO-modified titania, J. Colloid Interface Sci. 357 (2011) 223–228.

[20] S.-S. Chang, H.-J. Lee, H.J. Park, Photoluminescence properties of spark-processed CuO, Ceram. Int. 31 (2005) 411–415.

[21] A.M. Bazargan, S.M.A. Fateminia, M.E. Ganji, M.A. Bahrevar, Electrospinning preparation and characterization of cadmium oxide nanofibers, Chem. Eng. 155 (1-2) (2009) 523–527.

[22] T.D.N. Phan, E.W. Shin, Morphological effect of TiO_2 catalysts on photocatalytic degradation of methylene blue, J. Ind. Eng. Chem. 17 (2011) 397–400.

[23] S. Zhang, Z. Chen, Y. Li, Q. Wang, L. Wan, Photocatalytic degradation of methylene blue in a sparged tube reactor with TiO_2 fibers prepared by a properly two-step method, Catal. Commun. 9 (2008) 1178–1183.

[24] C. Karunakaran, G. Abiramasundari, P. Gomathisankar, G. Manikandan, V. Anandi, Cu-doped TiO_2 nanoparticles for photocatalytic disinfection of bacteria under visible light, J. Colloid Interface Sci. 352 (2010) 68–74.

[25] P.K. Stoimenov, R.L. Klinger, G.L. Marchin, K.J. Klabunde, Metal oxide nanoparticles as bactericidal agents, Langmuir 18 (2002) 6679–6686.

[26] K. Sunada, T. Watanabe, K. Hashimoto, Bactericidal activity of copper-deposited TiO_2 thin film under weak UV light illumination, J. Photochem. Photobiol. A 156 (2003) 227–233.